Supplemental Material for:

Room-temperature relaxor ferroelectricity and photovoltaic effects in tin titanate directly deposited on Si substrate

Radhe Agarwal[1], Yogesh Sharma[2,3], Siliang Chang[4], Krishna C. Pitike[5], Changhee Sohn[3], Serge M. Nakhmanson[5], Christos G. Takoudis[4,6], Ho Nyung Lee[3], Rachel Tonelli[7], Jonathan Gardner[7], James F. Scott[8], Ram S. Katiyar[1], and Seungbum Hong[2,9*]*

[1]Department of Physics and Institute for Functional Nanomaterials, University of Puerto Rico, San Juan, PR 00931, USA

[2]Material Science Division, Argonne National Laboratory, Lemont, IL 60439, USA

[3]Oak Ridge National Laboratory, Oak Ridge, Tennessee 37831, United States

[4]Department of Chemical Engineering, University of Illinois at Chicago, Chicago, Illinois 60607, USA

[5]Department of Materials Science and Engineering, Institute of Materials Science, University of Connecticut, Storrs, Connecticut 06269, USA

[6]Department of Bioengineering, University of Illinois at Chicago, Chicago, Illinois 60607, USA

[7]School of Chemistry, University of St. Andrews, St. Andrews, UK

[8]School of Physics and Astronomy, University of St. Andrews, St. Andrews, UK

[9]Department of Materials Science and Engineering, KAIST, Daejeon 34141, Republic of Korea

[*]Corresponding authors: sharmay@ornl.gov and seungbum@kaist.ac.kr

XRD measurements:

X-ray diffraction (XRD) measurements were carried out to study the structural characteristics of our thin films. Figure S1 (a) depicts the observed XRD patterns for Pt/$SnTiO_3$/Si thin film and Si substrate. XRD data reveals that the film is single-phase ferroelectric perovskite $SnTiO_3$ with different crystallographic orientations. Reflections from Si substrate and Pt-electrodes were marked separately, where the peaks corresponding to Pt (ICSD#52250) have been represented in blue color in XRD patterns. Peaks corresponding to $SnTiO_3$ have been indexed accordingly in XRD pattern. The peaks were assigned using a pattern simulated from crystallographic information files from the Inorganic Crystal Structures Database (ICSD) # 186724 [1]. The cell dimensions were modified and preferential orientation modeled in CrystalDiffract to obtain a match with the peak in the observed data. We observed several orientations of (100), (101), (011), and (211) grains and c/a ratios of these are 1.061, 1.144, 1.146, and 1.036 respectively. The reason that several $SnTiO_3$ peaks have multiple labels and overlap; is because $SnTiO_3$ lattice has slight tetragonal distortion and c and a lattice spacing are ca. 1% different. The (101) orientation has the lattice parameters: a = 3.60 Å, b = 3.80 Å and c = 4.12 Å. The (011) orientation has the lattice parameters: a = 3.84 Å, b = 3.84 Å and c = 4.40 Å. The (211) orientation has the lattice parameters: a = 3.97 Å, b = 3.78 Å and c = 4.11 Å. The (100) orientation has the lattice parameters: a = 3.84 Å, b = 3.84 Å and c = 4.07 Å. Moreover, (011) peak of $SnTiO_3$ can be well resolved from the stronger "forbidden" (002) line of the Si, as depicted in the high resolution XRD pattern near 2θ =32.5 deg. (Fig. S1 (b)).

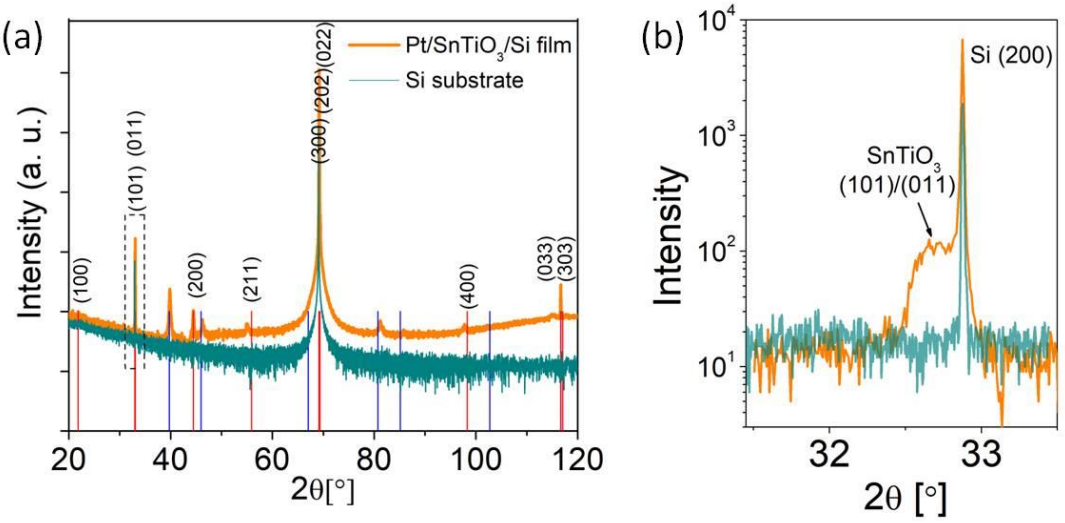

Figure S1 (a) XRD patterns of the Pt/$SnTiO_3$/Si film and Si substrate. Peaks for Pt and $SnTiO_3$ are shown in blue and red color respectively. (b) Higher resolution XRD pattern around the (200) Bragg peak of Si (marked in (a)), indicating (011) perovskite peak of $SnTiO_3$.

Capacitance-Voltage (CV) measurements in Pt/$SnTiO_3$/Si and Pt/$SnTiO_3$/Si/$SnTiO_3$/Pt

We have performed capacitance measurements on single MOS (Pt/$SnTiO_3$/Si)) and two back to back connected MOS (Pt/$SnTiO_3$/Si/$SnTiO_3$/Pt) (top-top) based capacitor structures of $SnTiO_3$ film. In case of single MOS structure, capacitance-voltage (C–V) curve becomes asymmetrical with respect to the polarity of the applied voltage, and the capacitance drastically decreased under positive bias (Fig. S2(a)). Conventionally, in a p-type semiconductor (p-Si in our case), the depletion layer in the semiconductor forms at positive bias [2]. This depletion layer contributes to an additional capacitance in the series with that of the ferroelectric, resulting in decrease in total capacitance at positive voltages. The reason why the two peaks in C–V for Fig. S2(a) is shifted to the negative bias voltage is because the depleted layer in p-Si creates a top to bottom electric field. However, the presence of two capacitance peaks attests to the fact that we are observing ferroelectric switching even in the MOS structure [3]. More interestingly, we observed the presence of two capacitance peaks (maxima) in more symmetric way for the case of two back to back connected MOS structure (Fig. S2(b)). Again, these peaks can be associated with the maxima present in the well-known butterfly shaped C–V characteristic obtained in the case of metal-ferroelectric-metal structures [4]. We believe that the capacitance peaks observed in the C–V curve of $SnTiO_3$ film are associated to polarization switching. Thus, the C–V measurements also

revealed a true ferroelectric property of our $SnTiO_3$ films.

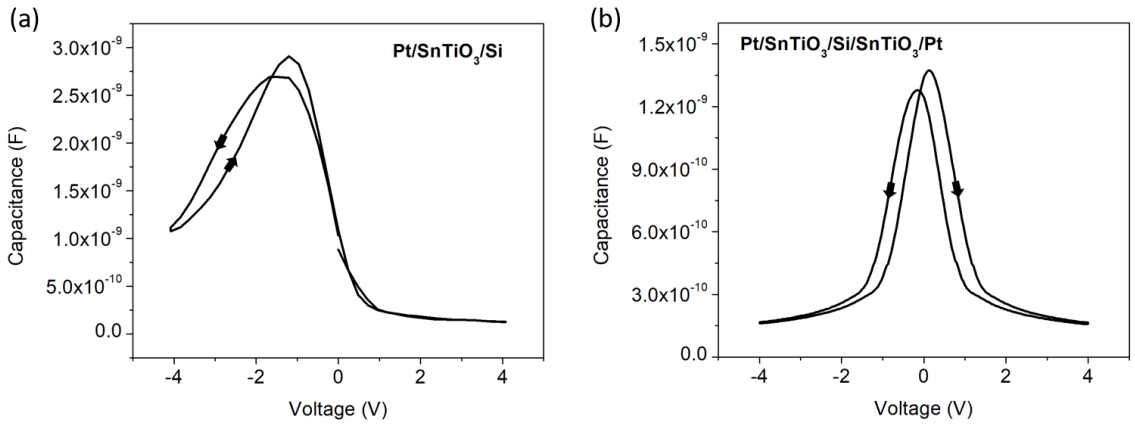

Figure S2: C–V curves of (a) $Pt/SnTiO_3/Si$ and (b) $Pt/SnTiO_3/Si/SnTiO_3/Pt$ capacitor structures of $SnTiO_3$ measured at 30 kHz with an ac probing signal of 200 mV.

Temperature dependent P-E hysteresis loops and PUND measurements

Figure S3 (a) shows the temperature dependent P–E hysteresis loop measured at 25 kHz. We observed stable ferroelectric polarization below freezing temperature (up to 420 K). Figure S3 (b) shows the remnant polarization as a function of applied voltage derived using PUND measurements. Triangular pulses of 25 µS width with 2 S delay were used for PUND measurements, as shown in the inset of Fig. S3 (b).

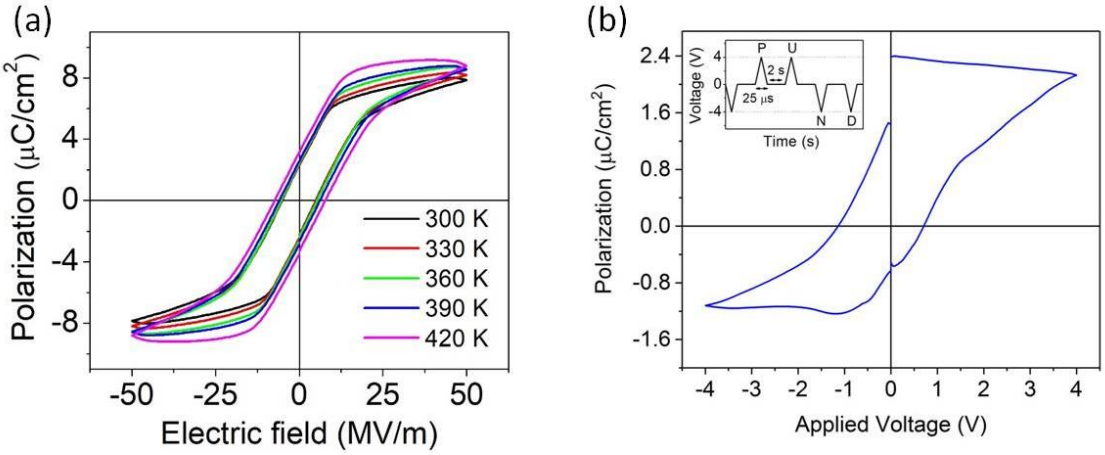

Figure S3: (a) Temperature dependence of P–E hysteresis loop (at 25 kHz) and (b) remnant polarization loop obtained from subtracting nonswitched polarization from switched polarization as a result of typical PUND measurement.

Photocurrent transient measurement:

Photocurrent (J_{SC}) value was recorded under continuous white light illumination in time duration of 120 seconds, shown in Fig. S4. Variation in J_{SC} could be explained by contribution of trap levels.

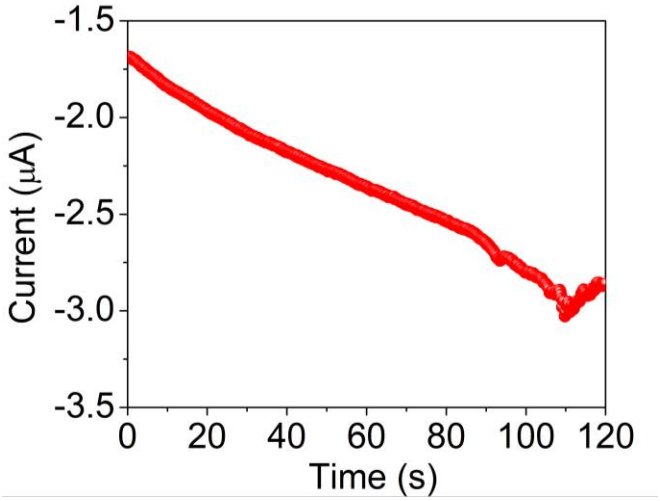

Figure S4: Variation in J_{SC} under continuous white light illumination of 120 seconds.

UV-assisted photovoltaic measurements:

$SnTiO_3$ thin films also showed photosensitivity in ultraviolet (UV) region. I–V curves under dark and UV light (wavelength of ~360 nm) illumination are shown in Fig. S5a. Fig. S5b and Fig. S5c show time dependence of photocurrent and photovoltage under multiple UV light on-off cycles. Moreover, incident light with above bandgap photon energy will be absorbed in the shallow region under the surface. It can be explained in terms of penetration depth and can be found using Beer-

Lambert law [5]. For UV illumination, it is about 21 nm and the value of absorption coefficient was considered to be about 0.048 nm^{-1}.

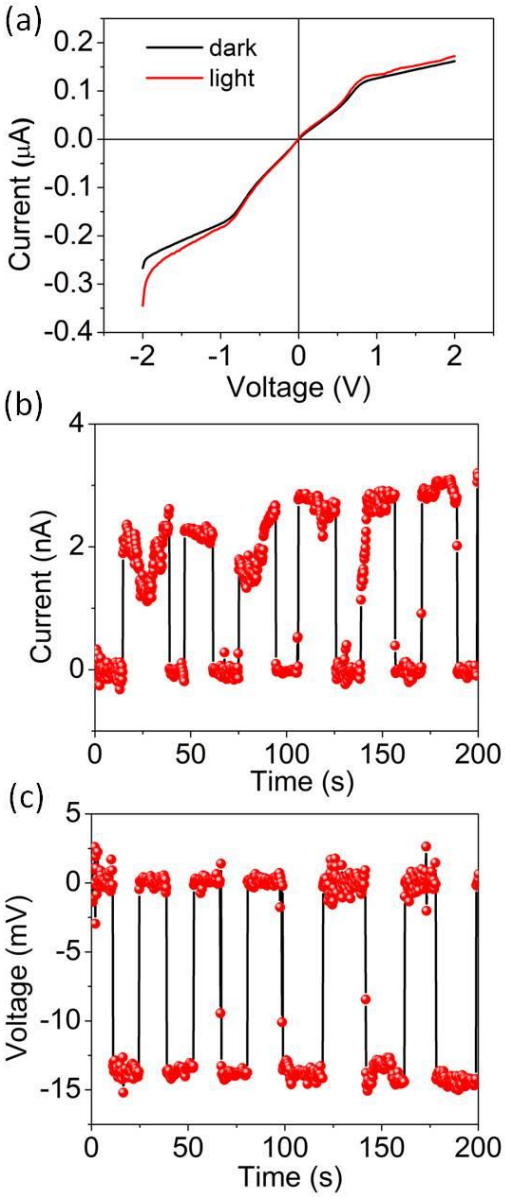

Figure S5: (a) I–V characteristics measured on Pt/$SnTiO_3$/p-Si/$SnTiO_3$/Pt capacitor in dark and under UV light illumination. Time dependence of (b) J_{SC} and (c) V_{OC} measured under multiple on/off light cycles.

Photovoltaic measurements under red light illumination:

I–V curves under dark and red light (wavelength of ~650 nm) illumination. We have used a red light-laser pointer for this measurement. As can be seen from the figure S6, a negligible contribution from p-Si substrate was observed on photovoltaic current.

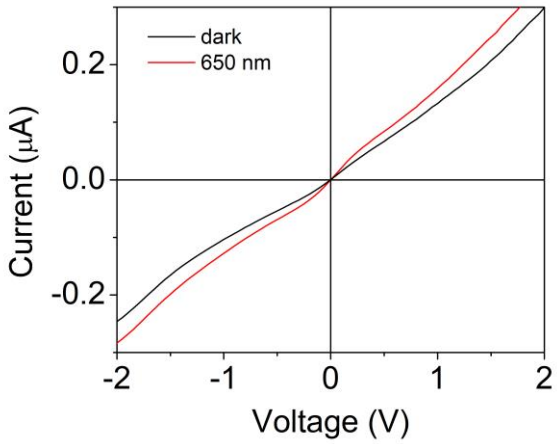

Figure S6: (a) I–V characteristics measured on Pt/$SnTiO_3$/p-Si/$SnTiO_3$/Pt capacitor in dark and under red light illumination.

Band gap tuning via tensile strain in $SnTiO_3$ films:

To elucidate the dependence of the optical band gap on the epitaxial strain induced by the substrate, the strain dependence of electronic properties of $SnTiO_3$ was studied using DFT calculations. Figure S7 shows the evolution of the valence-band maximum (VBM) and conduction-band minimum (CBM) energy levels of epitaxially strained $SnTiO_3$ computed with LDA (dashed lines) and HSE (solid lines) exchange correlation functionals. The data is shown for the epitaxial strain ε in the range of ± 2 (negative and positive values represent compression and tension, respectively). We observe the band-gap increasing from 2.175 eV, at $\varepsilon = 0$ to

2.655 eV, at $\varepsilon = +1\%$. An abrupt change in the band gap value happens between $\varepsilon = 0\%$ and $\varepsilon = +0.33\%$, as the system transitions from *P4mm* to *Cm* symmetry. The mechanism of the band gap opening is attributed to hybridization between Ti d_{xy} and O p_x orbitals at Γ point [6].

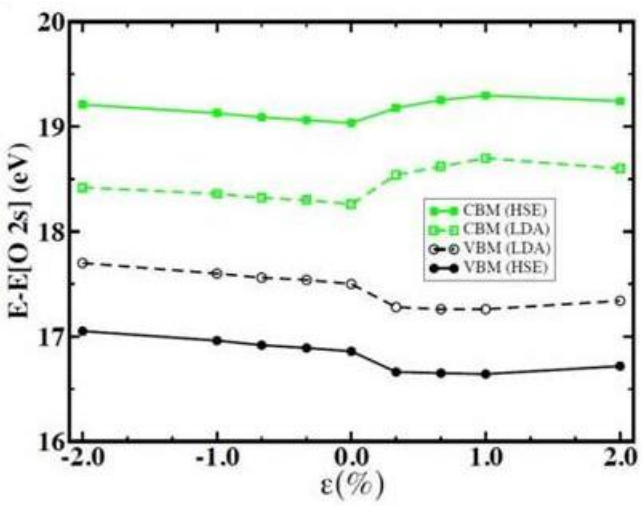

Figure S7: Calculated CBM and VBM values using LDA and HSE. In the latter case, a band gap of 2.175 eV is obtained for compressive and zero strains (*P*4*mm* phase), which increases to 2.655 eV in polar monoclinic *Cm* phase stabilized by tensile misfit strain. The location of the CBM and VBM energy levels is referenced with respect to the low-lying O 2*s* state, which is assumed to be undisturbed by any structural distortions.

REFERENCES

1. M.F.M. Taib, M.K. Yaakob, A. Chandra, A.K. Arof, M.Z.A. Yahya, *Effect of Pressure on Structural, Electronic and Elastic Properties of Cubic (Pm3m) $SnTiO_3$ Using First Principle Calculation*, Adv. Mat. Res. **501**, 342-346 (2012).
2. L. Pintilie, C. Dragoi, R. Radu, A. Costinoaia, V. Stancu, and I. Pintilie, *Temperature induced change in the hysteretic behavior of the capacitance-voltage characteristics of*

Pt–ZnO–Pb($Zr_{0.2}Ti_{0.8}$)O_3–PtPt–ZnO–Pb($Zr_{0.2}Ti_{0.8}$)O_3–Pt heterostructures, Appl. Phys. Lett. **96**, 012903 (2010).

3. W. Choi, S. Kim, Y. W. Jin, S. Y. Lee, and T. D. Sands, *Capacitance-voltage modeling of metal-ferroelectric-semiconductor capacitors based on epitaxial oxide heterostructures*, Appl. Phys. Lett. **98**, 102901 (2011).
4. L. Pintilie, M. Lisca, and M. Alexe, *Polarization reversal and capacitance-voltage characteristic of epitaxial Pb(Zr,Ti)O_3Pb(Zr,Ti)O_3 layers*, Appl. Phys. Lett. **86**, 192902 (2005).
5. M. Alexe, D. Hesse, *Tip-enhanced photovoltaic effects in bismuth ferrite*, Nat. Commun. **2**, 256 (2011).
6. W. D. Parker, J. M. Rondinelli, S. M. Nakhmanson, *First-principles study of misfit strain-stabilized ferroelectric $SnTiO_3$*, Phys. Rev. B **84**, 245126 (2011).